IOP Conf. Series: Materials Science and Engineering **267** (2017) 012034 doi:10.1088/1757-899X/267/1/012034

Investigation of Counter-Rotating Wind Turbine Performance using Computational Fluid Dynamics Simulation

V A Koehuan[1, 2*], Sugiyono[1] and S Kamal[1]

[1]Department of Mechanical and Industrial Engineering, Faculty of Engineering, Gadjah Mada University, Yogyakarta, Indonesia.
[2]Department of Mechanical Engineering, Faculty of Science and Engineering, Nusa Cendana University, Kupang 85001, Indonesia.

[*)] Corresponding author: verdy_koehuan@yahoo.com

Abstract. Investigation of the dual rotor counter-rotating wind turbine (CRWT) performance using non-dimensional parameters of the rotor diameter ratio and the rotor axial distance ratio against the characteristics of power coefficient with tip speed ratio (TSR) as input parameters have been successfully carried through CFD simulation. CFD simulation used *k-e* turbulence realizable with hexahedral meshing to predict the CRWT performance to the rotor diameter ratio of $D_1/D_2 < 1$, $D_1/D_2 = 1$ and $D_1/D_2 > 1$ and rotor axial distance ratio with the s826 airfoil that has been applied to the single rotor wind turbine. The best CRWT performance obtained on the rotor diameter ratio of $D_1/D_2 = 1.0$ with the peak power coefficient of 0.5219 or increased to $\Delta C_{P,\,max} = 16.49\%$ from the single rotor. CRWT performance through the addition of rotor axial distance ratio showed the power coefficient of the front rotor continued to rise closely to the single rotor performance while the rear rotor will continue to decline. However, the overall CRWT performance were relatively stable after the ratio of the distance $Z/D_1 = 0.5$ with the peak power coefficient of 0.5348 or increased to $\Delta C_{P,\,max} = 19.37\%$.

1. Introduction

Smart model of the three blades of horizontal axis wind turbine (HAWT) is known as counter-rotating wind turbine (CRWT) with the double rotor, rotating on the same axis in the opposite direction which has successfully presented the findings are interesting in parentheses recent years. The CRWT which have two rotors with the same diameter or different diameter at the same time, drive an alternator whose aerodynamic performance is better than the single rotor. Rotor with large size is placed in front and small one is placed behind it or otherwise with the rotational speed of the rotor is the synchronous moving alternator [1]. Energy conversion efficiency of turbines called wind turbine power coefficient for the dual rotors are theoretically better than a single rotor wind turbine (SRWT), where peak power coefficient of the single rotor from the theory of momentum (Betz limit), is 59.3%, Eggleston et al. [2]. Meanwhile, according to Newman [3] based on actuator disc theory, dual rotor wind turbine without any losses has maximum power coefficient 16/25 (64%).

[1] To whom any correspondence should be addressed.

Ushiyama et al. [4], through experimental studies on dual rotor wind turbine with a diameter ratio of $D_1/D_2 = 0.6$ (D_1front rotor diameter and rear rotor diameter D_2) indicated that the power coefficient of counter-rotating turbine was better than co-axial and single rotor, while the co-axial turbines best performance of the rotor with two blades. Lee et al. [5] through free wake vortex lattice method also showed the counter-rotating turbine with a diameter ratio of $D_1/D_2= 1$ performance was better than the single rotor and co-axial. Yuan et al. [6] and Ozbay et al. [7] showed the same results by studying the effect of rotation direction of dual rotor wind turbine through laboratory-scale experiments with a diameter ratio of $D_1/D_2 = 1$ and the axial separation ratio $Z/D_1 \geq 0.7$ (Z is axial distance of the two rotors) on the 2MW atmospheric wind turbine conditions of boundary layer.

Experiments and numerical analysis (quasi-steady strip method) of the counter-rotating wind turbine with power output of 30 kW have a front rotor diameter of 5.5 m (D_1) and the rear rotor of 11 m (D_2) or ($D_1/D_2 = 0.5$) with the ratio of the distance $Z/D_1 = 0.5$ indicated an increase in power output of 9% [8]. Furthermore, this study followed by Kumar et al. [9] through variation within the front and the rear rotor (diameter ratio of 0.5) for converting power optimization gained a 9.67% increase in the maximum power at a distance ratio of 0.65. Lee et al. [10] through numerical analysis with a modified blade element momentum theory in CRWT best performance on the diameter ratio of 0.4 and TSR = 8. Rosenberg, et al. [11] and followed by Moghadassian et al. [12] studied the design parameters of the counter-rotating wind turbine with the use of the similar airfoil to the single rotor and kept fixed the rear rotor TSR = 7.55. This study shows that the aerodynamic performance CRWT 10.08% is better than a single rotor with a diameter ratio of 0.25 and axial distance ratio 0.8. Shen et al. [13] using CFD, EllipSys3D Solver combined with the actuator line method, for predicting the CRWT performance to diameter ratio $D_1/D_2 = 1$ at TSR = 5.81, were compared with the experiment of Nordtank 500 kW. The results of this study show an increased annual energy production to 43.5% and the peak power coefficient of 0.5. Lee et al. [14] through a combination of methods blade element momentum theory and momentum, improvements were made to the design parameters of a single rotor and counter-rotating wind turbine as the pitch angle, and rotor rotation obtained the CRWT performance with $D_1/D_2 = 1$ is 12% higher than the single rotor. Usui et al [15] with a tandem rotor use diameter ratio of 1.19 and a ratio of the distance of 0.08 through optimization of the blade profile and blade angle has obtained an increase in turbine efficiency.

This study aims to investigate the performance of double rotor with counter-rotating wind turbines by using non-dimensional parameters of rotor diameter ratio and rotor axial distance ratio against the characteristics of power coefficient with tip speed ratio (TSR) as input parameters using CFD simulations. Various types of the blade (airfoil) has been used for the design and analysis of the aerodynamic performance of CRWT, where each of these studies was conducted separately to the diameter ratio, distance ratio, and tip speed ratio (TSR). CRWT performance of the various studies conducted on the rotor diameter ratio $D_1/D_2< 1$, $D_1/D_2 = 1$ or $D_1/D_2> 1$ with the axial distance and a certain blade to calculate the best CRWT performance at maximum conditions. This phenomenon is very interesting for further investigation to diameter ratio of $D_1/D_2< 1$, $D_1/D_2 = 1$ and $D_1/D_2> 1$ and the rotor axial distance ratio, the CRWT is in the best performance with the use of a particular type of blade in a fairly wide range of tip speed ratio. Blade models used in the CFD simulation for investigating the performance of CRWT is a single rotor wind turbine from the experimental of the Blind test program [16] [17].

2. Numerical Method

2.1. Blade geometry and parameters study

Blade model used in this study is a single rotor wind turbine blade developed by Krogstad et al. [16] and Bartl et al [17] as well as several other researchers on the Blind test program. The turbine rotor blade with a rotor diameter of 0.944 m used a series airfoil S826 issued by NREL (National Renewable Energy Laboratory). Figure 1 shows the blade used in this study and the non-dimensional parameters of rotor diameter ratio and the ratio of the axial distance of two rotors presented in Table 1

and Table 2. The front rotor diameter and operating conditions in this study maintained the same as the single rotor, while the blade geometry such as the number of blades, pitch angle, the front rotor and rear rotor solidity set as a control variable where the value remains constant.

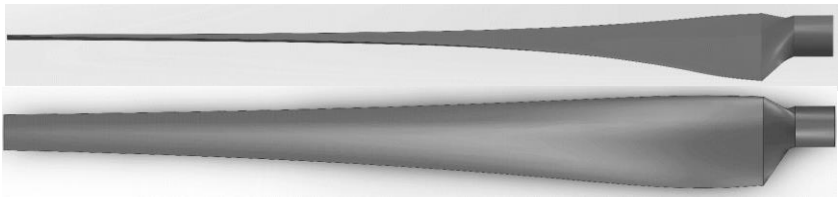

Figure 1. Blade model for counter-rotating wind turbine (CRWT).

Table 1. Parameters of rotor diameter ratio to axial distance ratio $Z/D_1 = 0.25$.

Parameters	Font (SRWT)	Rear				
		DR_1	DR_2	DR_3	DR_4	DR_5
rotor diameter, m	0.944	1.888	1.259	0.944	0.755	0.629
diameter ratio, D_1/D_2		0.5	0.75	1.0	1.25	1.5

Table 2. Parameters of rotor axial distance ratio.

Parameter	DZ_1	DZ_2	DZ_3	DZ_4	DZ_5	DZ_6	DZ_7	DZ_8
axial distance, m	0.1888	0.236	0.2832	0.3776	0.472	0.708	0.944	1.416
axial distance ratio, Z/D_1	0.2	0.25	0.3	0.4	0.5	0.75	1.0	1.5

2.2. Boundary conditions and meshing

Design and operational conditions of the single rotor turbine with a rotor diameter of 0.944 m that has peak power coefficient $C_{P,\,max} = 0.468$ at TSR 6 were applied to CRWT. The Numerical model used is the model with 1/3 of the domain (Figure 2) by assuming periodicity at the interface of cross-defined interfaces. While the mesh configuration is done through the process of volume, decomposition around the blade easily forms with hexahedral mesh element type using Gambit software. The single rotor turbine has 1.32 million of mesh nodes while CRWT follows the pattern of the single rotor with keeping the mesh density around the surface of the blade as shown in Figure 3.

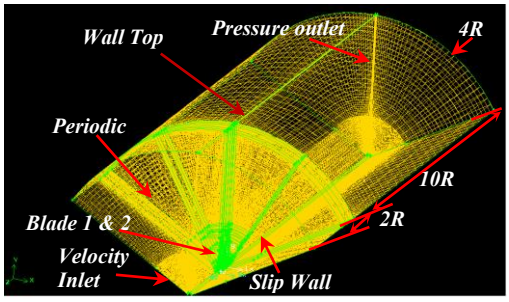

Figure 2. Meshing and computation domain, for rotor radius R = 0,472 m.

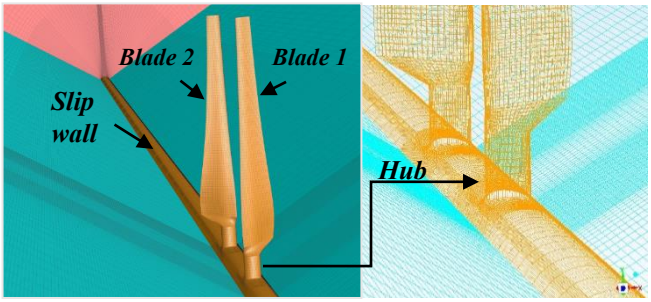

Figure 3. Surface mesh at slip wall and blade surface of the counter-rotating wind turbine.

2.3. Turbulent model

Determination of turbulence models depends on several considerations such as the physical characteristics of the flow, the experimental results for certain problems, the accurate level, the performance of existing computer and the time which are available for simulation. Turbulent model RANS (Reynolds-averaged Navier-Stokes) for incompressible and steady flow condition used by Taha et al. [18] is a model of turbulence *k-e* realizable, non-equilibrium pressure gradient was applied in this study.

Turbulent kinetic energy k and the dissipation rate of ε obtained from the general equation of fluid flow are the Reynolds-averaged Navier-Stokes (RANS) equations, where $\left(-\rho\overline{u_i'u_j'}\right)$ Reynolds stresses with components of speed, $u_i = \bar{u}_i + u_i'$,

$$\frac{\partial}{\partial t}(\rho k)+\frac{\partial}{\partial x_i}(\rho k u_i)=\frac{\partial}{\partial x_j}\left[\left(\mu+\frac{\mu_t}{\sigma_k}\right)\frac{\partial k}{\partial x_j}\right]+G_k+G_b-\rho\varepsilon-Y_M+S_k \quad (1)$$

$$\frac{\partial}{\partial t}(\rho \varepsilon)+\frac{\partial}{\partial x_i}(\rho \varepsilon u_i)=\frac{\partial}{\partial x_j}\left[\left(\mu+\frac{\mu_t}{\sigma_\varepsilon}\right)\frac{\partial \varepsilon}{\partial x_j}\right]+C_{1\varepsilon}\frac{\varepsilon}{k}\left(G_k+C_{3\varepsilon}G_b\right)-C_{2\varepsilon}\rho\frac{\varepsilon^2}{k}+S_\varepsilon \quad (2)$$

Where G_k is the generation of turbulent kinetic energy due to the average speed gradient, G_b is turbulent kinetic generation due to buoyancy, Y_M represents the contribution due to compressibility and $k=\overline{0.5\left(u_i'u_j'\right)}$ is the turbulent kinetic energy. $C_{1\varepsilon}$, $C_{1\varepsilon}$, and $C_{1\varepsilon}$ are constants; σ_k and σ_ε are Prandtl turbulent numbers for k and ε. The turbulent viscosity μ_t are calculated from combining k and ε with $\mu_t=\rho C_\mu\frac{k^2}{\varepsilon}$, Where C_μ is a constant. The constants used in the above formula taken based on the default [19].

2.4. Numerical solution method

The numerical solution is done by the finite volume technique for the nonlinear differential equations Navier-Stokes into a set of algebraic equations using pressure-based solver. Type of pressure-based solver is used with absolute velocity formulations, while the coupled algorithm solution scheme is used for pressure-velocity coupling. In the iterative procedure, the method of solution for the completion of the pressure equation used second order, while for momentum and turbulent equations used QUICK scheme, which, according to the hexahedral mesh type was used in order to enhance the accuracy. The present work was done using a CFD code called Fluent that run in parallel on a personal computer with an Intel Core i3 4130 CPU, 16GB memory, VGA graphics card NVIDIA GeForce GT 730 2GB.

3. Results and discussion

3.1. Validation of the numerical model

The numerical model validation and the composition of the mesh is used in the simulation model of the single rotor wind turbine by RMSE (root mean square error) to compute errors that occur at power coefficient and thrust coefficient measurement reported by Bartl and Sætran [12]. The turbine power coefficient (C_P) which is the result of dividing the mechanical power output (P_{out}) and the total power in the wind flow (P_{in}) for the rotor swept area (A) was given. This analysis is formulated as follows,

$$C_P=\frac{P_{out}}{P_{in}}=\frac{Q.W}{\frac{1}{2}\rho V_0^3 A} \quad (3)$$

$$C_T=\frac{T_{out}}{T_{in}}=\frac{T_{out}}{\frac{1}{2}\rho V_0^2 A} \quad (4)$$

Torque output, Q and thrust output, T_{out} on the rotor was obtained from the CFD simulation results. Figure 4 and Figure 5 show comparisons of power coefficient and thrust coefficient of the single rotor wind turbine between CFD simulation and measurement data respectively. CFD simulation performed with turbulence model *k-ε* realizable has a peak power coefficient at TSR = 6 with $C_{P,\,max}$ = 0.448 or

RMSE value of 2.0% which was lower than the measurement data reported by Bartl and Sætran [12]. CFD simulation results shown by the power coefficient are close enough to experiment on low TSR (RMSE value of 0.85%), but at high tend to widen (RMSE value of 25.72%). The results shown by the thrust coefficient were very close to the data measured by the average value of RMSE were 2.53 %.

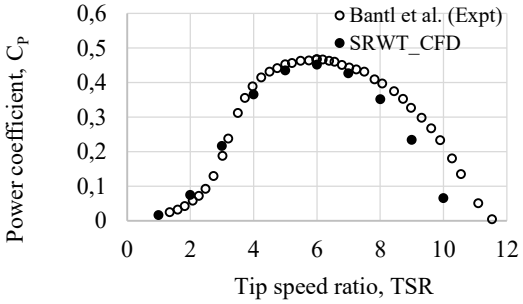

Figure 4. Comparison of SRWT power coefficient between CFD simulation and the experimental results.

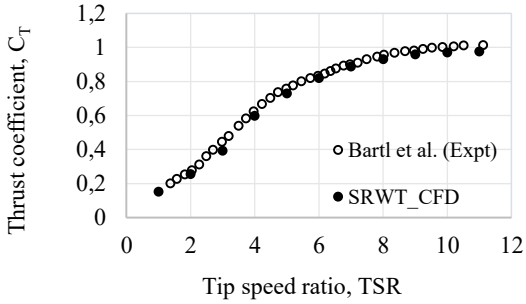

Figure 5. Comparison of SRWT Thrust coefficient between CFD simulation and the experimental results.

3.2. CRWT performance to rotor diameter ratio

Investigation of double rotor counter-rotating wind turbine performance through power coefficient characteristics with input parameters according to the single-rotor operating conditions were on tip speed ratio (TSR) between 1 and 11. The CFD simulations were performed using a constant speed of rotor rotation, which means that the front rotor and rear rotor rotation is kept constant with the ratio $n_2/n_1 = 0.6$ (n_1 and n_2 front rotor and rear rotor rotation respectively). Simulation parameters such as boundary conditions, the solution methods, and control solution, as well as the density of mesh nodes around the blade surface, made it equal to each variable in the rotor diameter and rotor axial distance of CRWT. While the convergence criteria for residual monitoring was set to 10^{-6} for all simulated parameters.

Comparison of the CRWT performance against SRWT from CFD simulations with variations of rotor diameter ratios performed at a rotor axial distance ratio of $Z/D_1 = 0.25$ for the range of tip speed ratios will be presented in two categories. Firstly, the increase in turbine power coefficient at the peak operating condition normalized by the SRWT expressed as $C_{P,\,max\,(CRWT)}/C_{P,\,max\,(SRWT)}$. The second is the increase in overall CRWT power coefficient that could be improved against SRWT at the range of TSR. From articles, review, the performance of CRWT tended to be partially related to the rotor diameter ratio was presented just for the peak performance with tip speed ratio (TSR) on its design condition. As we know that wind turbines are operated under atmospheric conditions, where natural freestream and design conditions will change with varied TSR ranges. Therefore, the performance of wind turbines must also be analysed for a wider TSR range so that turbine operations become more representative. The overall CRWT power coefficient would be obtained from the difference in the area that is formed by the curve of power coefficient and range of relative TSR. Figure 6 shows the power coefficient curve depicts a trend line by the second order polynomial agree well with the CFD result. Where the extent of this area is calculated by integrating the positive value of the power coefficient of relative tip speed ratio given in the input parameters. The area for representing the CRWT total power coefficient was normalized by SRWT which is presented as $A\_C_{P,\,CRWT}/A\_C_{P,\,SRWT}$. While the relative tip speed ratio (λ_R) is calculated based on the relative tip speed between the front rotor and rear rotor to the free stream flow, Usui et al. [15].

Comparison of the power coefficient between CRWT and SRWT with variations of rotor diameter ratio of CFD simulation results in Figure 6 shows the overall CRWT performance was better than SRWT. The peak power coefficient of the front rotor on $D_1/D_2 = 0.5$ and $D_1/D_2 = 0.75$ moved away from its operating conditions (TSR = 6) to TSR = 7 and TSR = 5 respectively, while for $D_1/D_2 = 1.0$ and $D_1/D_2 > 1.0$ stayed at TSR = 6. The maximum CRWT performance obtained on diameter ratio of

D_1/D_2 = 1.0 (DR_3) with a maximum power coefficient of 0.5219 or increase of normalization of 1.1649 times SRWT ($\Delta C_{P,\ max}$ = 16.49%) at relative TSR = 9.6, while based on relative TSR the normalized total power coefficient is 1.8732 times higher than SRWT. From the CFD simulation, the higher CRWT performance in the range of diameter ratio D_1/D_2< 1.0 is D_1/D_2 = 0.5 (DR_1) and for diameter ratio D_1/D_2> 1.0 is D_1/D_2 = 1.25 (DR_4). Figure 6a and 6b show the CRWT performance on DR_1 and DR_4 with a maximum power coefficient of 12.45% and 8.54% at relative TSR = 10.99 and 8.88 respectively, while based on relative TSR the normalized overall power coefficient is 2.2067 for DR_1 and 1.7402 for DR_4 which is higher than SRWT. It appears that both front rotor power coefficient of DR_1 and DR_4 tended to rise and move closer to the single rotor (SRWT) to provide a positive contribution to overall CRWT performance.

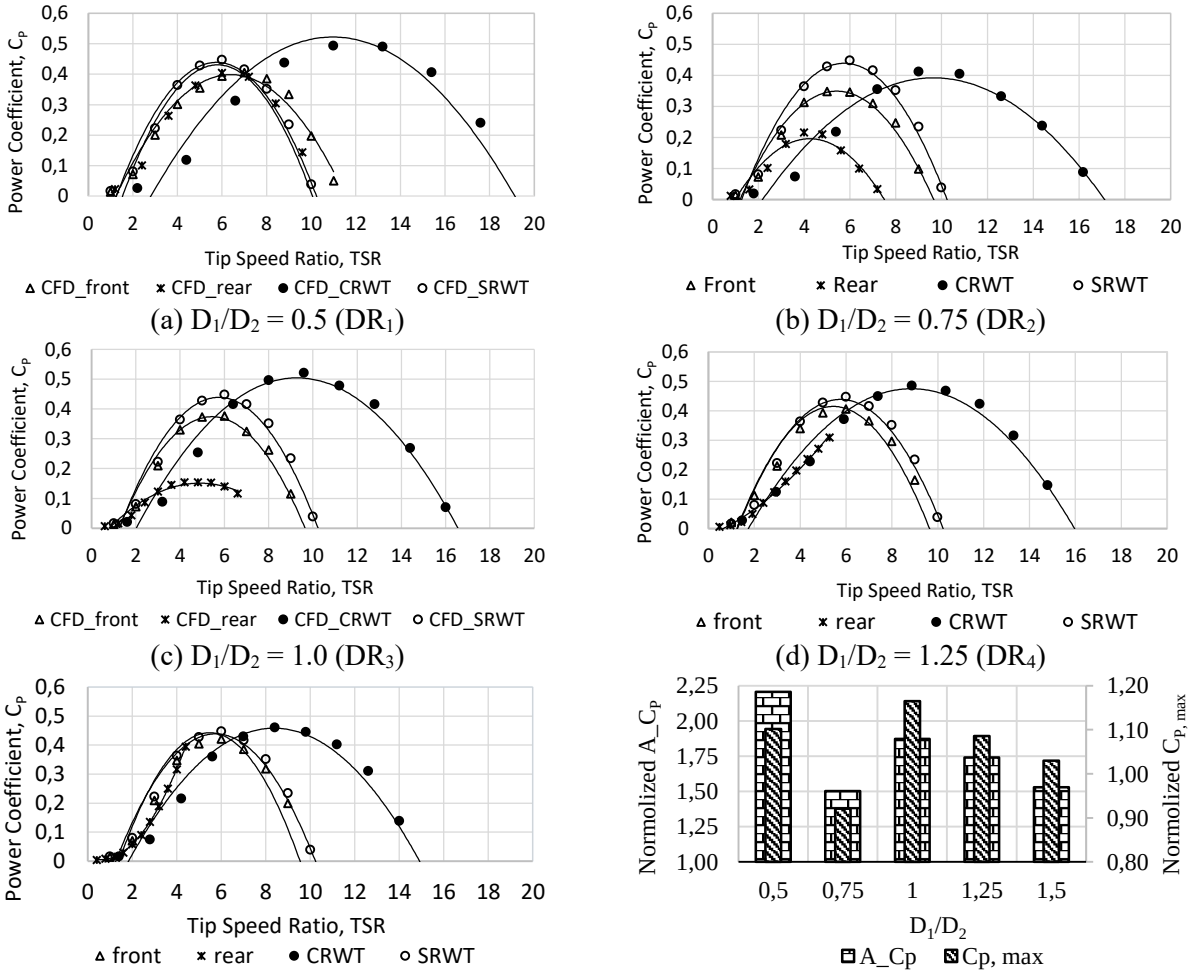

(a) D_1/D_2 = 0.5 (DR_1) (b) D_1/D_2 = 0.75 (DR_2)

(c) D_1/D_2 = 1.0 (DR_3) (d) D_1/D_2 = 1.25 (DR_4)

(e) D_1/D_2 = 1.5 (DR_5) (f) Enhancement of power coefficient

Figure 6. Comparison of power coefficient between CRWT and SRWT to tip speed ratios with a variation of rotor diameter ratio parameters at a rotor separation ratio of Z/D1 = 0.25.

The effects of the rear rotor diameter variation on the CRWT performance are when the rear rotor diameter is larger than the front rotors (D_1/D_2<1.0), then the CRWT performance increase with the addition of the rear rotor diameter is visible from both rising power coefficient for the front rotor and rear rotors. When the rear rotor diameter is smaller than the front rotor (D_1/D_2> 1.0), then the CRWT performance tends to drown if the rear rotor diameter was continuously scaled and characterized by the decrease of overall CRWT power coefficient (front and rear), although there was an increase in

front of rotor power coefficient. While CRWT achieves the maximum performance at $D_1/D_2 = 1.0$ which is geometrical when the front rotor diameter fixed and rear rotor diameter or the sweep area becomes larger ($D_1/D_2<1.0$), because the sweep area were proportional to power so increasing it the input power become higher. Conversely, when the rear rotor diameter becomes smaller ($D_1/D_2> 1.0$), the output power becomes low so that it effectively reduced turbine power coefficient. Because the rear rotor is operated in the wake of the front so that the rear rotor performance tends to be lower than the front rotors, although there is an increase in overall CRWT performance compared to SRWT. However, the diameter ratio of $D_1/D_2 = 0.5$, there is an increase on the rear rotor power coefficient than front rotor itself. The rear rotor diameter was two times greater than the front rotor or half of its blade length is not hindered by the front rotor and contacted directly to free stream so the loss due to the interference of flow from the front rotor is reduced. CRWT performance decline by the decreasing of the rear rotor diameter due to the its overall length on the interference of the front rotor. Flow disturbance resulted in a change of the magnitude and direction of inflow to the blade from design conditions, especially on the blade tip that produced vortex and separation on the blade surface.

3.3. CRWT performance to rotor axial distance ratio

CRWT performance against rotor axial distance ratio is shown in Figure 7 and Figure 8 with $D_1/D_2 = 1.0$, indicates that the overall power coefficient increases along with the increasing distance of the two rotors of $Z/D_1 = 0.2$ (DZ_1) to $Z/D_1 = 0.5$ (DZ_5). Performance of CRWT on $Z/D_1 = 0.2$ (DZ_1) is $\Delta C_{P,\,max}$ = 11.77% and $Z/D_1 = 0.5$ (DZ_5) with $\Delta C_{P,\,max}$ = 19.37% was better than single rotor. Furthermore, CRWT performance on the rotor axial separation ratio between $Z/D_1 = 0.5$ (DZ_5) and $Z/D_1 = 1.5$ (DZ_8) shows the front rotor power coefficient continued to increase with the addition of rotor axial distance to the single rotor performance. However, the opposite of the rear rotor power coefficient tends to fall but increased in CRWT performance and it was relatively stable after rotor axial distance ratio of Z/D1 = 0.5. By increasing the axial distance between two rotors, interference on the rear rotor was reduced and the velocity of the front rotor is recovered that increases the front rotor power coefficient, Lee et al. [14]. CFD prediction shown in Figure 8 indicated that interference of both front and rear rotors are quite stronger below the axial distance ratio of $Z/D_1 = 0.5$ as well as the lower front rotor power coefficient. However, after the axial distance ratio of $Z/D_1 = 0.5$, the power coefficient the front rotor was increased slightly and the rear rotor continues to decrease to $Z/D_1 = 1.5$, because of velocity recovery behind the front rotor and velocity deficit of the rear rotor decrease slowly.

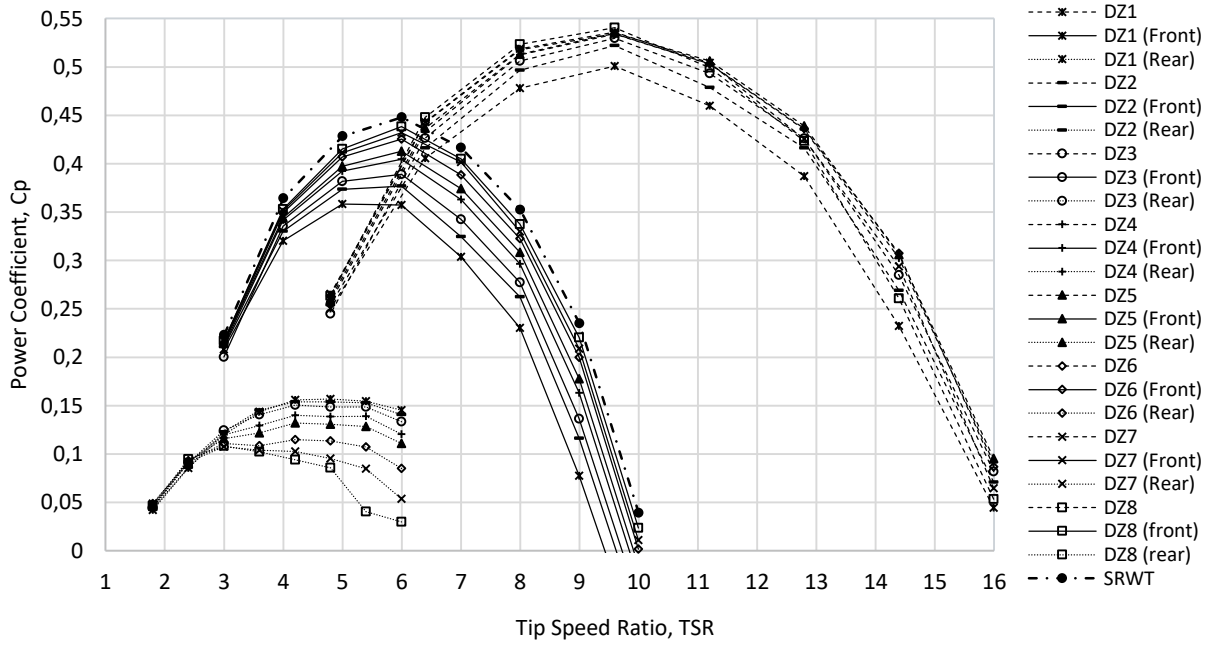

Figure 7. Power coefficient variation for CRWT, front and rear rotors against SRWT according to rotor axial distance ratio with diameter ratio $D_1/D_2 = 1.0$.

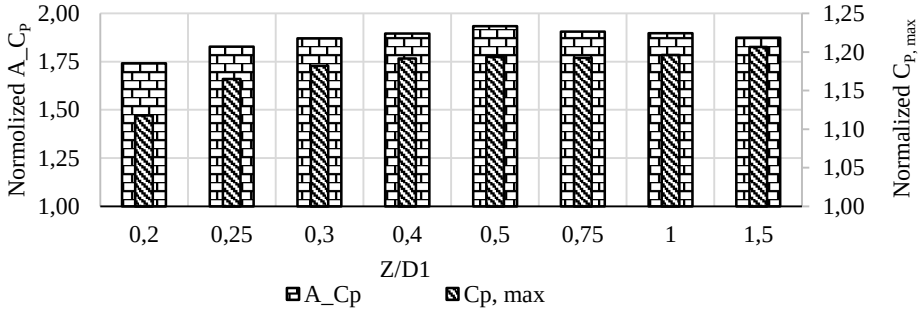

Figure 8. Enhancement of normalized maximum power coefficient and the normalization of overall power coefficient for CRWT against SRWT according to rotor axial distance ratio with diameter ratio $D_1/D_2 = 1.0$.

4. Conclusion

Investigation of counter-rotating wind turbines (CRWT) performance through power coefficient characteristics with a wide range input parameter of tip speed ratio, rotor diameter ratio and the ratio of the axial distance of the rotor has been successfully carried through CFD simulations. On the peak condition, CRWT performance obtained on diameter ratio of $D_1/D_2 = 1.0$ with a maximum power coefficient of 0.5219 or increased $\Delta C_{P,\,max} = 16.49\%$, while based on relative TSR the normalized total of power coefficient is 1.8732 times higher than SRWT. Evidence from CFD simulation results show the highest total CRWT power coefficient is in the diameter ratio $D_1/D_2 = 0.5$ (DR_1) and not in $D_1/D_2 = 1.0$ (DR_3) which has the highest peak power coefficient. CRWT performance to distance ratio shows the front rotor power coefficient continues to increase with the addition of rotor axial distance to near single rotor performance, the opposite of the rear rotor power coefficient tends to fall resulting in the increase of CRWT performance which was relatively stable after rotor axial separation ratio $Z/D_1 = 0.5$.

5. References

[1]. Kanemoto T and Galal A M 2006 Development of Intelligent Wind Turbine Generator with Tandem Wind Rotors and Double Rotational Armatures (1st Report, Superior Operation of Tandem Wind Rotors) *JSME Inter. Journal* **Series B 49(2)** 450–457

[2]. Eggleston D M and Stoddard F 1987 *Wind Turbine Engineering Design* (New York: Van Nostrand Reinhold)

[3]. Newman B G 1983 Actuator-disc Theory for Vertical-axis Wind Turbines *Journal of Wind Engineering and Industrial Aerodynamics* **15(1-3),** pp.347–355

[4]. Ushiyama I, Shimota T, Miura Y 1996 An experimental study of the two-staged wind turbines, *Renewable Energy* **9(1)** p 909-912.

[5]. Lee S, Kim H, and Lee S S, 2010 Analysis of aerodynamic characteristics on a counter-rotating wind turbine *Current Applied Physics* **10(2)**pp. S339–S342.

[6]. Yuan W, Ozbay A, Tian W and Hu H 2013 An Experimental Investigation on the Effects of Turbine Rotation Directions on the Wake Interference of Wind Turbines *51st AIAA Aerospace Sci. Meeting including the New Horizons Forum and Aerospace Exposition*(Grapevine Texas: AIAA) p 607

[7]. Ozbay A, Tian W, and Hu H 2014 An Experimental Investigation on the Aeromechanics and Near Wake Characteristics of Dual-Rotor Wind Turbines (DRWTs) *32nd ASME Wind Energy Sym.*, 13-17 January 2014 (National Harbor Maryland: AIAA 2014-1085)

[8]. Jung S N, No T S, and Ryu K 2005 Aerodynamic performance prediction of a 30 kW counter-rotating wind turbine system *Renewable Energy* **30(5)** 631–644

[9]. Kumar P S, Abraham A, Bensingh R J, and Ilangovan S 2013 Computational and Experimental analysis of a Counter-Rotating Wind Turbine System *Journal of Scientific and Industrial Research* **72** May pp. 300–306
[10]. Lee S, Kim H, Son E, and Lee S S 2012 Effects of design parameters on aerodynamic performance of a counter-rotating wind turbine *Renewable Energy* **42**pp. 140–144.
[11]. Rosenberg A, Selvaraj S, and Sharma A 2014 A Novel Dual-Rotor Turbine for Increased Wind Energy Capture *Journal of Physics*: Conference Series **524** (012078) p 11(IOP Publishing).
[12]. Moghadassian B, Rosenberg A, Hu H, and Sharma A 2015 Numerical Investigation of Aerodynamic Performance and Loads of a Novel Dual Rotor Wind Turbine *33rd Wind Energy Symposium 5-9 January 2015* (Kissimmee Florida: AIAA SciTech) p 14
[13]. Shen W Z, Zakkam V A K, Sørensen J N, and Appa K 2007 Analysis of Counter-Rotating Wind Turbines *Journal of Physics*: Conference Series **75** (012003) p 10
[14]. Lee S, Son E, and Lee S S 2013 Velocity interference in the rear rotor of a counter-rotating wind turbine *Renewable Energy* **54**pp. 235–240.
[15]. Usui Y, Kubo K, Kanemoto T 2012 Intelligent Wind Power Unit with Tandem Wind Rotors and Armatures (Optimization of Front Blade Profile) *Journal of Energy and Power Eng.***6**pp. 1791-1799.
[16]. Krogstad P Å and Eriksen P E 2013 Blind test calculations of the performance and wake development for a model wind turbine, *Renewable Energy* **50** pp. 325-333.
[17]. Bartl J and Sætran L 2017 Blind test comparison of the performance and wake flow between two in-line wind turbines exposed to different turbulent inflow conditions *Wind Energy Science* **2(1)**, pp.55-76.
[18]. Taha Z, Sugiyono, Sawada T 2010 A comparison of computational and experimental results of Wells turbine performance for wave energy conversion *Applied Ocean Research* **32** pp. 83-90
[19]. Ansys Fluent 12.0 Documentation.

Acknowledgement
The authors thank the Ministry of Research, Tech., and Higher Education of the Republic of Indonesia and LPPM University of Nusa Cendana for supporting this research and paper through The Grant 2016.